iScience

CellPress
OPEN ACCESS

Article

Cell surface morphology mimicking nano-bio platform for immune cell stimulation

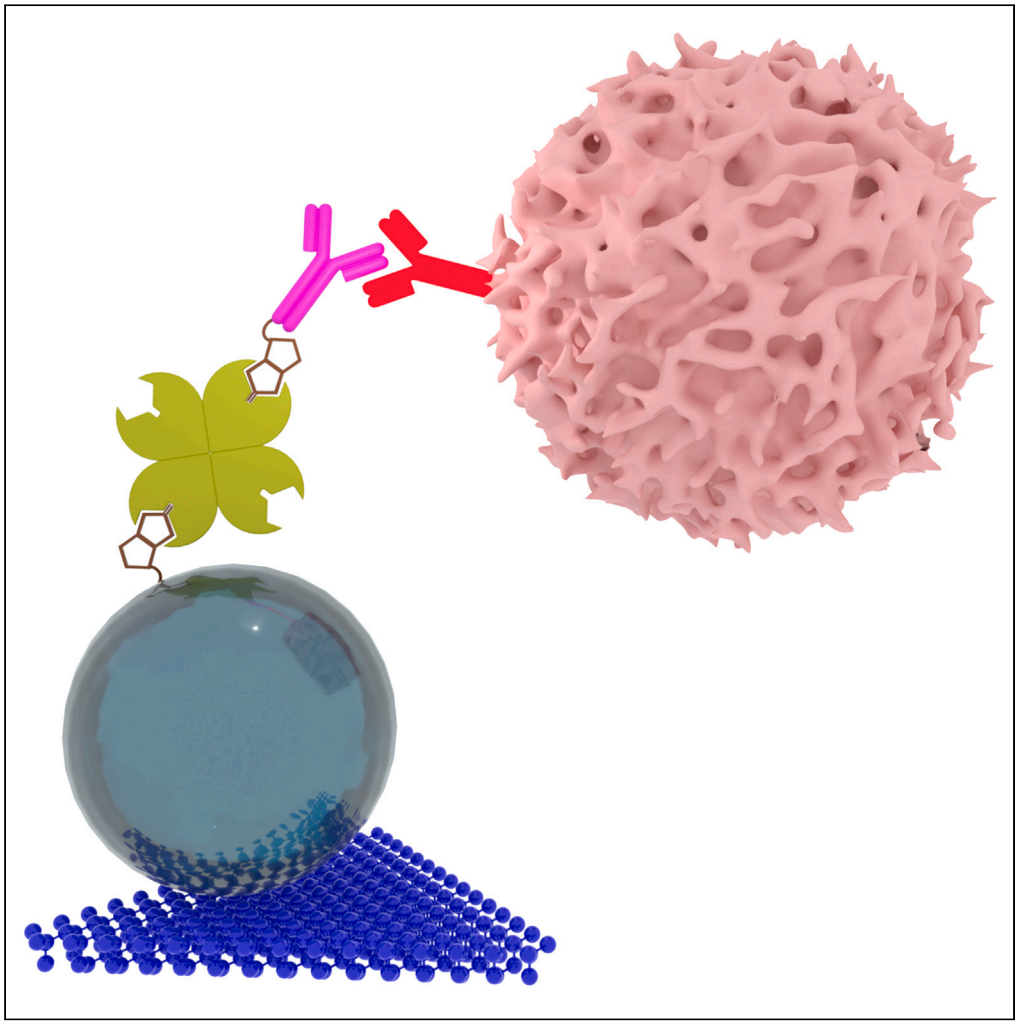

Beena Varghese, José Alfredo González-Navarro, Valentino Libero Pio Guerra, ..., Tejaswini Rama Bangalore Ramakrishna, Marek Cebecauer, Petr Kovaříček

petr.kovaricek@vscht.cz

Highlights

Nanoparticle-ligand platform to mimic antigen-presenting cell microvilli

Specific T cell activation by naturally presented antibodies

Suppressed non-specific activation in fluorescence microscopy imaging

Broad benchtop applicability without advanced nanofabrication equipment

Varghese et al., iScience 27, 111033
November 15, 2024
https://doi.org/10.1016/j.isci.2024.111033

iScience

CellPress
OPEN ACCESS

Article

Cell surface morphology mimicking nano-bio platform for immune cell stimulation

Beena Varghese,[1] José Alfredo González-Navarro,[2] Valentino Libero Pio Guerra,[1] Margarita Faizulina,[1] Daria Artemieva,[1,2] Tomáš Chum,[2] Tejaswini Rama Bangalore Ramakrishna,[2] Marek Cebecauer,[2] and Petr Kovaříček[1,3,*]

SUMMARY

Studying the complex realm of cellular communication and interactions by fluorescence microscopy requires sample fixation on a transparent substrate. To activate T cells, which are pivotal in controlling the immune system, it is important to present the activating antigen in a spatial arrangement similar to the nature of the antigen-presenting cell, including the presence of ligands on microvilli. Similar arrangement is predicted for some other immune cells. In this work, immune cell-stimulating platform based on nanoparticle-ligand conjugates have been developed using a scalable, affordable, and broadly applicable technology, which can be readily deployed without the need for state-of-the-art nanofabrication instruments. The validation of surface biofunctionalization was performed by combination of fluorescence and atomic force microscopy techniques. We demonstrate that the targeted system serves as a biomimetic scaffold on which immune cells make primary contact with the microvilli-mimicking substrate and exhibit stimulus-specific activation.

INTRODUCTION

T cells are an essential part of the immune system protecting vertebrates from infection or cancer. Their misfunction may lead to diverse pathologies, e.g., immunodeficiency or autoimmunity diseases. T cells are activated and regulated through their characteristic surface receptors. T cell receptor (TCR) recognizes foreign patterns (antigens) in the form of the peptide-major histocompatibility complex (pMHC) on the surface of target cells called antigen-presenting cells (APCs). Productive interaction triggers an initial activation of signaling.[1] In almost all published T cell activation studies employing advanced fluorescence microscopy, the APC was represented by the optical surface (coverslip) and ligands restricted to the focal plane by direct immobilization on the glass or via a supported planar bilayer. In other words, T cells were always interacting with a flat surface in these experiments. Such arrangement is probably unlike the T cell interaction with APCs *in vivo*. Under physiological conditions, TCR present on microvilli or other membrane protrusions of T cells searches for pMHC with cognate antigens on a complex morphology of APCs. This may imply a different geometry of the TCR/pMHC (T cell/APC) interaction compared to a flat surface. Recently, diverse approaches were designed to enable pre-controlled stimulation of T cells with alternative ligand geometry. Among those, functionalized micropillars most closely mimic membrane protrusions of APCs.[2,3] These pillars, designed to track receptor-induced forces, have a diameter of 0.5–1 μm and are more reminiscent of larger membrane protrusions such as ruffles or filopodia. Other approaches focused primarily on the spacing between stimulating nodes (pMHC clusters, e.g., <5 nm gold beads[4]) or the shape and size of stimulating ligands (e.g., using DNA origami[5]). To our knowledge, no system was developed to mimic stimulation of T cells through pMHC on microvilli of APCs. However, earlier data indicate the involvement of microvilli on dendritic cells, master APCs in humans, in the activation of T cells.[6] Similar role of microvilli was described or predicted for other immune cells.[7–9]

Nanotechnology introduced a variety of objects with feasible sizes and functional advantages to mimic the geometry of microvilli.[10] Nanoparticles are broadly available in a variety of compositions, sizes, and surface functionalization. Metal nanoparticles, quantum dots, and polymer microbeads are among the most widely used materials exhibiting either bright fluorescence or, conversely, optical transparency.[11–13] The surface coating determines the dispersibility and stability in solvents as well as reactivity with other species. Frequently employed are inert and hydrophilic PEG chains. Desired specific reactivity is then introduced through diverse terminating groups such as carboxylic acid, thiol, azido, or amino groups.[14]

Here, we present a biomimetic platform to perform fluorescent microscopy imaging with living cells. We based the design on multilayer nano-bio platform for interactions with biological and cellular systems.[15] Differences in the nanomaterial and biomolecule composition in turn impose challenges on the specificity and atom economy of employed transformations, which add to the mundane request for high level of

[1]Department of Organic Chemistry, Faculty of Chemical Technology, University of Chemistry and Technology Prague, 166 28 Prague, Czechia
[2]Department of Biophysical Chemistry, J. Heyrovsky Institute of Physical Chemistry, Czech Academy of Sciences, Dolejškova 2155/3, 182 23 Prague, Czechia
[3]Lead contact
*Correspondence: petr.kovaricek@vscht.cz
https://doi.org/10.1016/j.isci.2024.111033

control over density and distribution homogeneity of the presented activators. We were motivated to develop a practical fluorescent microscopy platform mimicking accumulation of ligands on microvilli with minimal technological requirements for a broad use. We demonstrate the functionality of the developed platform by monitoring specific T cell activation using a cytosolic calcium-sensitive probe.

RESULTS AND DISCUSSION

Design

We have designed a platform based on conventional glass coverslips for fluorescence microscopy imaging to ensure compatibility with objective working distance limitation. Glass surface functionalization is most performed by commercial triethoxysilane anchors available in a variety of functional terminations, including (3-aminopropyl)triethoxysilane (APTES) to introduce amino groups on glass. Amines on the surface allow for both irreversible and reversible ligation of small molecule linkers through alkylation and imine condensation reactions, respectively. The reversible condensation with an aldehyde grafted to the surface brings several advantages and the dual reactivity of the functionalization agent has important consequences. Firstly, during the reaction of 4-(bromomethyl)benzaldehyde with the APTES treated substrate, the irreversible nucleophilic substitution will eventually outcompete the reversible imine condensation. Secondly, both aldehyde and imine species on the surface are prone to react with amino-functionalized particles when in proximity to the surface. Thirdly, the thermodynamically governed ligation allows for chemoselective assays to confirm the nature of particle bonding to the surface as well as its "fixing" by mild and chemoselective reduction to a secondary amine. Finally, optimization of desired particle density on the surface is only dependent on the particle concentration in the supernatant solution, because the particle ligation to the surface is an equilibrium of multidentate binder-substrate interaction.[16]

This primary functionalization to readily available amino functionalized nanoparticles fulfill several roles in our design: (1) due to their size and curvature they mimic microvilli of a cell, which have finger-like structure with around 100 nm in diameter, (2) they increase spatial separation of the presented biomolecule from the surface and thus avoid the steric clashes,[17] and (3) the amino group is suitable for biomolecule linkage onto the nanoparticle. Two types of nanoparticles, Polybead Amino microspheres 0.10 μm polystyrene beads (PS, Polysciences) and Cd-based Amine Quantum Dots (QD, QSA580 Ocean NanoTech) were used in this study in different stages of platform development. Free surface amino groups on anchored nanoparticles were biotinylated and through tetravalent streptavidin functionalized for further attachment of desired molecules (e.g., stimulating ligands). In this work, biotinylated antibodies (anti-Hu CD3ε) were anchored to the particles to mimic pMHC at the tip of microvilli of APCs. Fluorescently labeled molecules were used in several stages of the development to visualize generated structures by imaging using a widefield microscope with a single-fluorophore sensitivity. An overview of the multilayer system design is presented in Scheme 1.

Chemical surface functionalization

The coverslip surface was activated by piranha treatment to increase hydroxyl groups[18] density for reaction with APTES.[19] This leads to a surface with pending amino groups. To link amino-functionalized particles to such a surface, a bifunctional linker is required. We have used 4-(bromomethyl)benzaldehyde featuring two reactive groups. The benzylic bromide is irreversibly replaced by N-nucleophiles, such as the pending NH_2 group from APTES functionalization, while the aldehyde forms imines with amine reversibly. The functionalization was monitored by measurement of contact angle (CA). "Piranha"-treated glass shows an immeasurably low contact angle which increases to 51° after APTES functionalization due to the contribution of propyl chains. After the reaction with 4-(bromomethyl)benzaldehyde, the contact angle increases further to 67° due to the hydrophobic nature of the benzaldehyde moiety. A summary of the basic characterization of chemically modified coverslips is shown in the Figure S1.

We attached two different types of amine functionalized particles, PS and QD, to the aldehyde-decorated glass surface of coverslips. PS are optically silent, do not interfere with the fluorescence imaging, and have diameter comparable to the microvilli size (*ca* 100 nm), which is ideal for the target of this work.[20] QD, on the other hand, are smaller (<5 nm) and feature intense well-defined luminescence without photobleaching, which is beneficial for optimization experiments.[21] QD were used during development of the platform for control experiments, while PS beads were the target system to mimic microvilli.

The surface bound aldehyde groups react with amine functionalities of nanoparticles to form an imine (C=N) linkage. This linkage has two major advantages. Its inherent dynamicity allows to discern non-specific sedimentation of particles on the surface from the desired covalent anchoring via chemoselective reactions. Moreover, the inherent dynamicity can be "frozen" by reduction with sodium cyanoborohydride to a stable secondary amine.[22] We have employed acetate buffer (pH 4.5) washing to remove non-bound particles. Acidic medium promotes hydrolysis of the imine linkage and protonates pendant amino groups both on the particle and the surface. This leads to Coulombic repulsion and as a result only particles covalently linked to the surface remain.

Particle density on the surface is an important parameter because crowded surface representation of antibodies would lead to a steric hindrance for cell receptor recognition. Relying on imine linkages, the ligation of particles to the surface is an equilibrium process, which can be controlled by a particle concentration in the applied dispersion. We have optimized the concentration of QD and PS dispersions to 10^{15} and 10^{10} particles/mL, respectively. After cyanoborohydride reduction and acetate buffer washing, the samples showed the desired particle density, 0.3–1 μm^{-2} on the surface, as characterized by atomic force microscopy (AFM), and for QDs also long-term fluorescence, thus demonstrating stability of the particle anchoring (Figure 1).[15] This density represents 10–80 particles per the area, which forms a contact site between a lymphocyte and the glass surface. It is within the range of expected microvilli contacts between a lymphocyte and a target cell.[6]

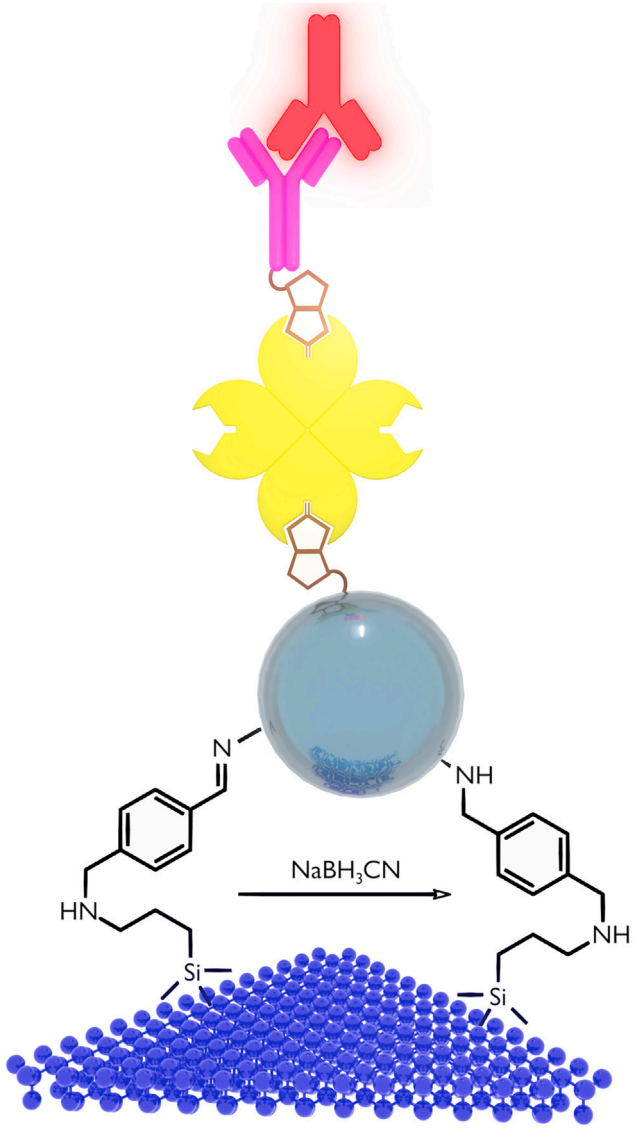

Scheme 1. Design and development of a biomimetic nano-platform for live-cell fluorescence microscopy mimicking microvilli presentation of ligands for immune cells

Chemical surface functionalization introduces reversible imine linkage for thermodynamic binding of (nano)particles, which is fixed by mild reduction. Biotin is covalently linked to the nanoparticle and binds to tetravalent streptavidin. Free binding sites are used by biotinylated ligands (e.g., antibodies) for stimulation of imaged cells.

Biomolecule immobilization

Attachment of signaling biomolecules to the particle surface was pursued via strong, specific biotin-avidin binding. First, the particle surface was biotinylated with 15 mM in aqueous solution of sulfo-NHS-biotin (30 min at room temperature [RT]), which reacts with pending NH_2 group forming a stable amide bond.[23] To confirm successful biotinylation, we have incubated both the QD and PS-decorated surface with 20 ng/mL Alexa Fluor 647-labeled streptavidin. In both cases, characteristic fluorescence of the dye was recorded in the micrograph (Figure 2). In contrast to QDs, the fluorescence signal of streptavidin was dramatically reduced upon photobleaching (Figure S3). Inherent QD signal, on the other hand, did not undergo photobleaching and their signal remains stable upon bleaching energies applied to the sample. The results are summarized in Figure S3. Using the fluorescently labeled streptavidin, we have optimized its concentration to 20 ng/mL in aqueous phosphate-buffered saline (PBS) with 0.5% bovine serum albumin (BSA, see STAR Methods, surface functionalization section for details).

To test the final step of the nano-bio platform functionalization, we have incubated the system with biotinylated anti-human CD3ε (MEM-57) antibody, which binds to the remaining sites of tetravalent streptavidin. The MEM-57 antibody binding was confirmed and visualized by complexation of this primary antibody with Alexa Fluor 647-labeled goat anti-mouse IgG antibody (secondary antibody). Fluorescence images of the

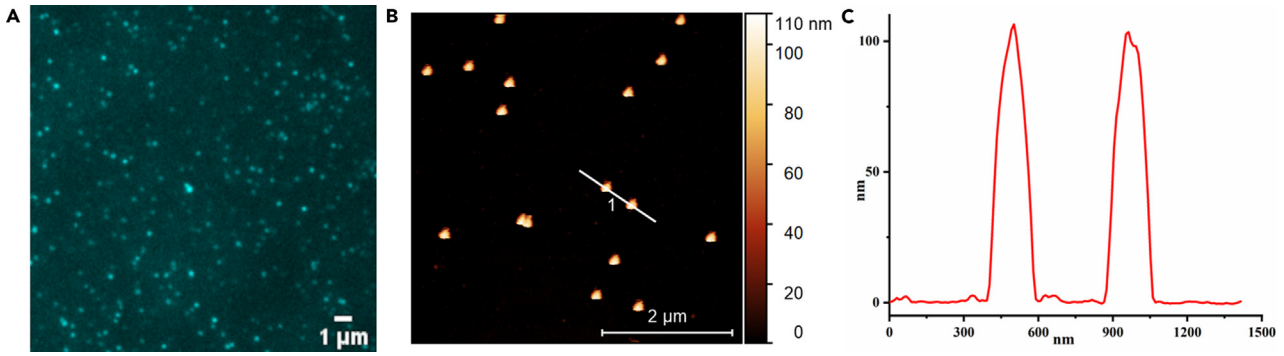

Figure 1. Characterization of coverslip functionalized with QDs and PS beads

(A) Fluorescence image of a coverslip surface with anchored QDs, excitation wavelength 405 nm, cut-off filter 525 nm, scale bar, 1 μm.

(B) AFM image of a coverslip surface with PS beads showing on average 0.7 PS bead per μm^2, scale bar, 2 μm.

(C) Height AFM profile of marked line in B showing particle height/size of 100 nm, i.e., similar to the microvilli diameter. See also Figure S2.

system after staining with the secondary antibody demonstrate successful formation of the fully functionalized nano-bio platform for stimulation of T cells (Figure 2). Photobleaching experiments were performed to confirm the presence of the organic dye—Alexa Fluor 647 (Figure S4).

Live-cell imaging of T cell activation on functionalized nano-bio platform

To demonstrate successful development of the platform for T cell activation, we monitored calcium mobilization upon receptor stimulation in the immortalized model of T cells (Jurkat E6 cell line, ATCC TIB-152[24]) expressing GCaMP6f genetically encoded calcium sensor.[25] Jurkat cells forming contact with nanobeads functionalized with activating anti-human CD3ε antibody exhibited transient, but strong increase in the intracellular calcium (Figure 3A; Videos S1, S2, and S3). Almost 60% of cells on the nano-bio platform with anti-human CD3ε antibody underwent

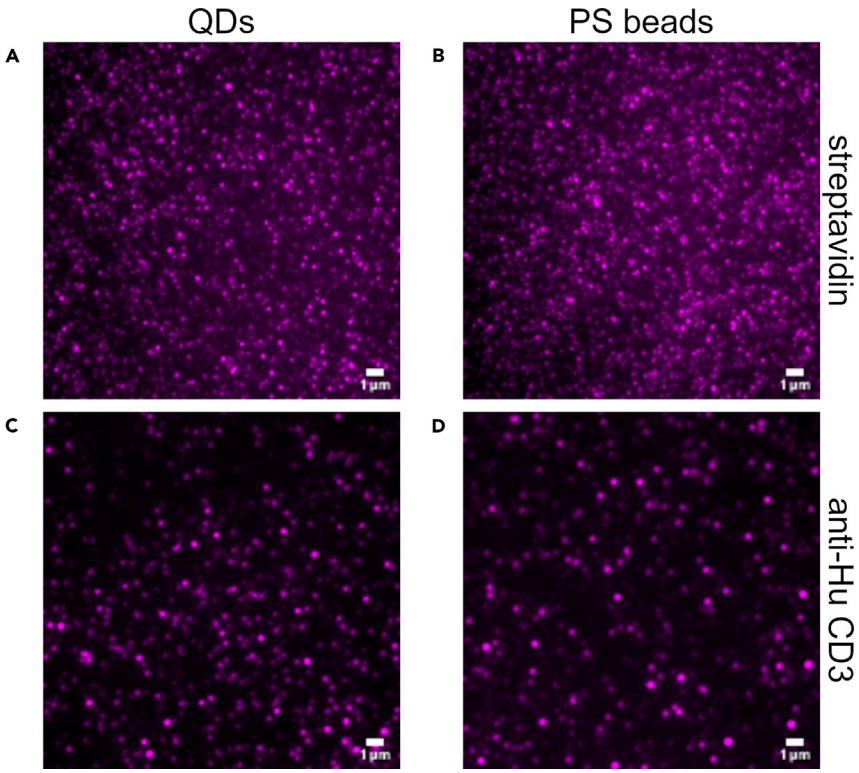

Figure 2. Fluorescent microscope images of nano-bio platform containing QDs and PS beads

(A–D) Visualization of QDs (A and C) and PS beads (B and D) on functionalized nano-bio platform by fluorescence imaging: (A) and (B) represents binding of Alexa Fluor 647-labeled streptavidin (see Scheme 1 for details); (C) and (D) represents binding of anti-Hu CD3ε biotin (mouse IgG) via non-labeled streptavidin and visualized by goat anti-mouse IgG Alexa Fluor 647-labelled secondary antibody. Scale bar in all images, 1 μm. See also Figures S3 and S4.

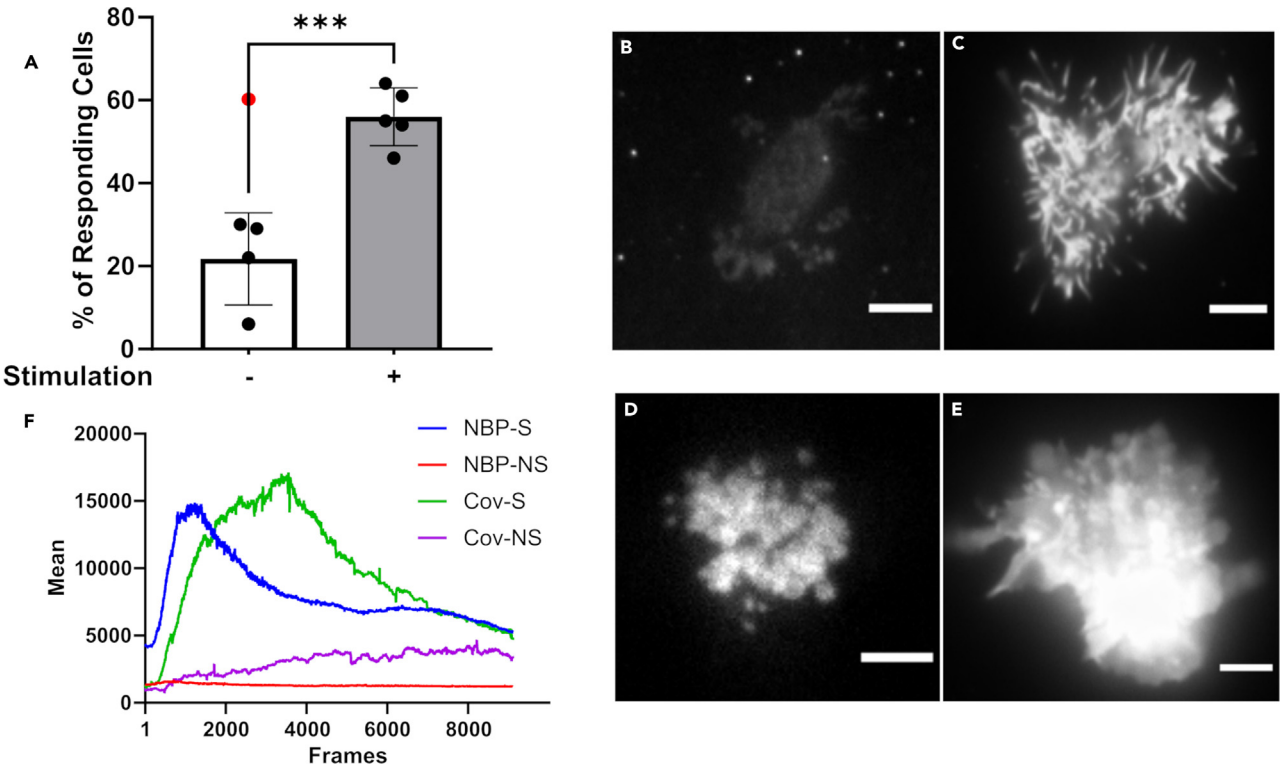

Figure 3. Overview of the Calcium response of Jurkat cells on nano-bio platforms

(A) Calcium response of Jurkat cells upon contact with the nano-bio platform containing QD lacking antibodies (-, negative control) (n = 370) or QD with anti-human CD3ε antibodies (MEM-57) (+, with stimulating antibody) (n = 218). The magnitude of the calcium response was calculated using the software CalQTrace.[29,30] Relative calcium response was calculated by an AI-based decision algorithm to classify individual cells as triggering (activated) or non-triggering (resting) upon contact with the modified surface and during 15 min of the measurement at 37°C. Statistical difference was assessed using unpaired t test (GraphPad Prism 9); ***$p < 0.001$. Dots in the graph represent independent measurement days. A red dot represents a value of an outlier. Data are presented as means ± S.E.M.

(B–E) Representative images of a Jurkat cell contact with non-stimulating (B) and stimulating (C) nano-bio platform. Similarly, images of Jurkat contact with non-stimulating (D) and stimulating (E) surface prepared using standard method of direct antibody immobilization (see STAR Methods). Cells were transfected with genetically encoded calcium sensor GCaMP6fu and imaged using total internal reflection fluorescence (TIRF) microscopy. Scale bar in all images, 3 μm. Movies of the live-cell imaging of Jurkat cell activated on nano-bio platform are in the Videos S1, S2, S3, S4, S5, S6, S7, S8, S9, S10, and S11.

(F) Graph showing changes in mean fluorescence intensity of the calcium sensor GCaMP6fu detected in single cells forming a contact with nano-bio platform (NBP) or coverslip (Cov) with stimulating (S) or non-stimulating (NS) surfaces (as in A–E). See also Figure S5.

activation whereas only approximately 20% of cells on the surface generated by omitting the last functionalization step with the antibody (negative control) exhibited a weak calcium mobilization (Figure 3B). This was probably caused by the mechanical stress upon T cell contact with the coverslip in the unmodified areas. The activation of Jurkat cells using nano-bio platform with anti-CD3 antibodies on beads was comparable to the previously employed stimulation mode,[26] in which direct immobilization of antibodies at the coverslip was used (Figure S5). Detailed image analysis demonstrates active engagement of membrane protrusions on the surface of Jurkat cells with the activating antibody on beads of the nano-bio platform (Figure 3C). No such preferred morphology was detected in cells stimulated with antibodies directly immobilized on the surface of coverslips (Figures 3B, 3D, and 3E; Videos S7, S8, and S9) or on non-stimulating surface (Videos S10 and S11) independent of its modification mode (Figures 3B, 3D, and 3E; Videos S4, S5, and S6). Quantitative analysis of calcium mobilization indicates more rapid response of Jurkat cells to antibodies on the nano-bio platform (NBP) compared to their direct immobilization at the coverslips (Cov)—Figure 3F. These data provide evidence that the newly developed nano-bio platform can induce local response to ligands by receptors accumulated at the tips of T cell microvilli as reported recently.[27,28]

Conclusions

The antibody-functionalized platform with T cell stimulating capacity has been fabricated through simple and straightforward protocols and a design schematically represented in Scheme 1. It combines the characteristics of "off-the shelf" availability, design versatility, and multiple interactions to achieve highly efficient T cell activation. The approaches to modulate antigen-specific T cell responses presented here are also meant to be used as a guideline to develop various immune cell stimulating or modulating that imitate diverse conditions of the human

immune system. In this work, we demonstrated principal function of our system by focusing on a nanopatterned T cell activating platform on an optical surface, which allows multiplexed imaging with selected ligands. Further development is required to combine stimulating particles with integral negative control or dual-target platform.

Limitations of the study

We have developed a biocompatible nanoplatform mimicking the intercellular specific activation of T cells with suppressed non-specific stress activation. The platform possibly can be used for other cell types; however, this was not verified in this study. Moreover, the specific anti-human CD3ε antibody was ligated via biotin-avidin binding, which is available for many other antigens, but we only explored a single type of stimulation of T cells and no stimulation with native ligands (such as peptide-MHCII) was tested due to the lack of specific ligands for the model cells used in this study.

RESOURCE AVAILABILITY

Lead contact

Further information and requests for resources and reagents should be directed to and will be fulfilled by the lead contact, Petr Kovaříček (petr.kovaricek@vscht.cz).

Materials availability

This study did not generate new unique reagents.

Data and code availability

Data

All data reported in this paper will be shared by the lead contact upon request.

Code

This paper does not report original code.

Final statement

Any additional information required to reanalyze the data reported in this paper is available from the lead contact upon request.

ACKNOWLEDGMENTS

The work was supported by the Czech Science Foundation grant no. 22-11299M "Reaction networks at phase interfaces for dynamic self-assembly". The team was also supported by the Experientia Foundation 2021 start-up grant. We acknowledge the support of the Dagmar Prochazkova Foundation of the University of Chemistry and Technology Prague. The work of J.A.G.N., D.A., T.C., T.R.B.R., and M.C. was also supported by the Czech Science Foundation grant no. 19-07043S.

AUTHOR CONTRIBUTIONS

Conceptualization, M.C. and P.K.; methodology, B.V., M.F., D.A., and T.R.B.R.; formal analysis, J.A.G.N. and T.C.; investigation, B.V., J.A.G.N., V.L.P.G., M.F., D.A., T.C., and T.R.B.R.; resources, M.C. and P.K.; witing – original draft, M.C. and P.K.; writing – review and editing, B.V., J.A.G.N., V.L.P.G., M.F., D.A., T.C., T.R.B.R., M.C., and P.K.; supervision, V.L.P.G., T.C., M.C., and P.K.; funding acquisition, M.C. and P.K.

DECLARATION OF INTERESTS

There is no conflict of interests to declare.

STAR★METHODS

Detailed methods are provided in the online version of this paper and include the following:

- KEY RESOURCES TABLE
- EXPERIMENTAL MODEL AND STUDY PARTICIPANT DETAILS
  - Cell lines
- METHOD DETAILS
  - Contact angle measurement
  - Atomic force microscopy
  - Fluorescence microscopy
  - Chemical reagents & solutions
  - Surface functionalization
- QUANTIFICATION AND STATISTICAL ANALYSIS
  - Large-scale calcium measurement

SUPPLEMENTAL INFORMATION

Supplemental information can be found online at https://doi.org/10.1016/j.isci.2024.111033.

Received: March 15, 2024
Revised: September 4, 2024
Accepted: September 23, 2024
Published: September 26, 2024

REFERENCES

1. Delcassian, D., Sattler, S., and Dunlop, I.E. (2017). T Cell Immunoengineering with Advanced Biomaterials. Integr. Biol. *9*, 211–222. https://doi.org/10.1039/c6ib00233a.
2. Jin, W., Tamzalit, F., Chaudhuri, P.K., Black, C.T., Huse, M., and Kam, L.C. (2019). T Cell Activation and Immune Synapse Organization Respond to the Microscale Mechanics of Structured Surfaces. Proc. Natl. Acad. Sci. USA *116*, 19835–19840. https://doi.org/10.1073/pnas.1906986116.
3. Bashour, K.T., Gondarenko, A., Chen, H., Shen, K., Liu, X., Huse, M., Hone, J.C., and Kam, L.C. (2014). CD28 and CD3 Have Complementary Roles in T-Cell Traction Forces. Proc. Natl. Acad. Sci. USA *111*, 2241–2246. https://doi.org/10.1073/pnas.1315606111.
4. Deeg, J., Axmann, M., Matic, J., Liapis, A., Depoil, D., Afrose, J., Curado, S., Dustin, M.L., and Spatz, J.P. (2013). T Cell Activation Is Determined by the Number of Presented Antigens. Nano Lett. *13*, 5619–5626. https://doi.org/10.1021/nl403266t.
5. Sun, Y., Sun, J., Xiao, M., Lai, W., Li, L., Fan, C., and Pei, H. (2022). DNA Origami–Based Artificial Antigen-Presenting Cells for Adoptive T Cell Therapy. Sci. Adv. *8*, eadd1106. https://doi.org/10.1126/sciadv.add1106.
6. Fisher, P.J., Bulur, P.A., Vuk-Pavlovic, S., Prendergast, F.G., and Dietz, A.B. (2008). Dendritic Cell Microvilli: A Novel Membrane Structure Associated with the Multifocal Synapse and T-Cell Clustering. Blood *112*, 5037–5045. https://doi.org/10.1182/blood-2008-04-149526.
7. Saltukoglu, D., Özdemir, B., Holtmannspötter, M., Reski, R., Piehler, J., Kurre, R., and Reth, M. (2023). Plasma Membrane Topography Governs the 3D Dynamic Localization of IgM B Cell Antigen Receptor Clusters. EMBO J. *42*, e112030. https://doi.org/10.15252/embj.2022112030.
8. Frey, T., Petty, H.R., and McConnell, H.M. (1982). Electron Microscopic Study of Natural Killer Cell-Tumor Cell Conjugates. Proc. Natl. Acad. Sci. USA *79*, 5317–5321. https://doi.org/10.1073/pnas.79.17.5317.
9. Kim, H.-R., and Jun, C.-D. (2019). T Cell Microvilli: Sensors or Senders? Front. Immunol. *10*, 1753.
10. Orbach, R., and Su, X. (2020). Surfing on Membrane Waves: Microvilli, Curved Membranes, and Immune Signaling. Front. Immunol. *11*, 2187. https://doi.org/10.3389/fimmu.2020.02187.
11. Perica, K., Kosmides, A.K., and Schneck, J.P. (2015). Linking Form to Function: Biophysical Aspects of Artificial Antigen Presenting Cell Design. Biochim. Biophys. Acta *1853*, 781–790. https://doi.org/10.1016/j.bbamcr.2014.09.001.
12. Luo, X., and Liu, J. (2022). Ultrasmall Luminescent Metal Nanoparticles: Surface Engineering Strategies for Biological Targeting and Imaging. Adv. Sci. *9*, 2103971. https://doi.org/10.1002/advs.202103971.
13. Eggermont, L.J., Paulis, L.E., Tel, J., and Figdor, C.G. (2014). Towards Efficient Cancer Immunotherapy: Advances in Developing Artificial Antigen-Presenting Cells. Trends Biotechnol. *32*, 456–465. https://doi.org/10.1016/j.tibtech.2014.06.007.
14. Samanta, D., and Sarkar, A. (2011). Immobilization of Bio-Macromolecules on Self-Assembled Monolayers: Methods and Sensor Applications. Chem. Soc. Rev. *40*, 2567–2592. https://doi.org/10.1039/c0cs00056f.
15. Wauters, A.C., Scheerstra, J.F., Vermeijlen, I.G., Hammink, R., Schluck, M., Woythe, L., Wu, H., Albertazzi, L., Figdor, C.G., Tel, J., et al. (2022). Artificial Antigen-Presenting Cell Topology Dictates T Cell Activation. ACS Nano *16*, 15072–15085. https://doi.org/10.1021/acsnano.2c06211.
16. Fasting, C., Schalley, C.A., Weber, M., Seitz, O., Hecht, S., Koksch, B., Dernedde, J., Graf, C., Knapp, E.-W., and Haag, R. (2012). Multivalency as a Chemical Organization and Action Principle. Angew. Chem., Int. Ed. Engl. *51*, 10472–10498. https://doi.org/10.1002/anie.201201114.
17. Gao, S., Guisán, J.M., and Rocha-Martin, J. (2022). Oriented Immobilization of Antibodies onto Sensing Platforms - A Critical Review. Anal. Chim. Acta *1189*, 338907. https://doi.org/10.1016/j.aca.2021.338907.
18. Demirel, G., Çaykara, T., Akaoğlu, B., and Çakmak, M. (2007). Construction of a Novel Multilayer System and Its Use for Oriented Immobilization of Immunoglobulin G. Surf. Sci. *601*, 4563–4570. https://doi.org/10.1016/j.susc.2007.06.034.
19. Miranda, A., Martínez, L., and De Beule, P.A.A. (2020). Facile synthesis of an aminopropylsilane layer on Si/SiO2 substrates using ethanol as APTES solvent. MethodsX *7*, 100931. https://doi.org/10.1016/j.mex.2020.100931.
20. Zhang, D.K.Y., Cheung, A.S., and Mooney, D.J. (2020). Activation and Expansion of Human T Cells Using Artificial Antigen-Presenting Cell Scaffolds. Nat. Protoc. *15*, 773–798. https://doi.org/10.1038/s41596-019-0249-0.
21. Franke, C., Chum, T., Kvíčalová, Z., Glatzová, D., Gentsch, G.J., Rodriguez, A., Helmerich, D.A., Herdly, L., Mavila, H., Frank, O., et al. (2022). Approach to Map Nanotopography of Cell Surface Receptors. Commun. Biol. *5*, 218. https://doi.org/10.1038/s42003-022-03152-y.
22. Spicer, C.D., Pashuck, E.T., and Stevens, M.M. (2018). Achieving Controlled Biomolecule–Biomaterial Conjugation. Chem. Rev. *118*, 7702–7743. https://doi.org/10.1021/acs.chemrev.8b00253.
23. Williams, E.H., Davydov, A.V., Motayed, A., Sundaresan, S.G., Bocchini, P., Richter, L.J., Stan, G., Steffens, K., Zangmeister, R., Schreifels, J.A., and Rao, M.V. (2012). Immobilization of Streptavidin on 4H–SiC for Biosensor Development. Appl. Surf. Sci. *258*, 6056–6063. https://doi.org/10.1016/j.apsusc.2012.02.137.
24. Weiss, A., Wiskocil, R.L., and Stobo, J.D. (1984). The Role of T3 Surface Molecules in the Activation of Human T Cells: A Two-Stimulus Requirement for IL 2 Production Reflects Events Occurring at a Pre-Translational Level. J. Immunol. *133*, 123–128.
25. Helassa, N., Zhang, X.h., Conte, I., Scaringi, J., Esposito, E., Bradley, J., Carter, T., Ogden, D., Morad, M., and Török, K. (2015). Fast-Response Calmodulin-Based Fluorescent Indicators Reveal Rapid Intracellular Calcium Dynamics. Sci. Rep. *5*, 15978. https://doi.org/10.1038/srep15978.
26. Glatzová, D., Mavila, H., Saija, M.C., Chum, T., Cwiklik, L., Brdička, T., and Cebecauer, M. (2021). The Role of Prolines and Glycine in the Transmembrane Domain of LAT. FEBS J. *288*, 4039–4052. https://doi.org/10.1111/febs.15713.
27. Kim, H.R., Mun, Y., Lee, K.S., Park, Y.J., Park, J.S., Park, J.H., Jeon, B.N., Kim, C.H., Jun, Y., Hyun, Y.M., et al. (2018). T Cell Microvilli Constitute Immunological Synaptosomes That Carry Messages to Antigen-Presenting Cells. Nat. Commun. *9*, 3630. https://doi.org/10.1038/s41467-018-06090-8.
28. Cai, E., Marchuk, K., Beemiller, P., Beppler, C., Rubashkin, M.G., Weaver, V.M., Gérard, A., Liu, T.L., Chen, B.C., Betzig, E., et al. (2017). Visualizing Dynamic Microvillar Search and Stabilization during Ligand Detection by T Cells. Science *356*, eaal3118. https://doi.org/10.1126/science.aal3118.
29. Barbieri, L. (2021). Quantitative Biophysical Methods to Study Immune Cell Mechanobiology (University of Oxford). https://ora.ox.ac.uk/objects/uuid:55fde4e5-7d84-4b14-a040-20cb96a5d52d.
30. Lee, A.M., Colin-York, H., and Fritzsche, M. (2017). CalQuo 2: Automated Fourier-space, population-level quantification of global intracellular calcium responses. Sci. Rep. *7*, 5416. https://doi.org/10.1038/s41598-017-05322-z.
31. Nečas, D., and Klapetek, P.G. (2012). An Open-Source Software for SPM Data Analysis. Open Phys. *10*, 181–188. https://doi.org/10.2478/s11534-011-0096-2.
32. Edelstein, A.D., Tsuchida, M.A., Amodaj, N., Pinkard, H., Vale, R.D., and Stuurman, N. (2014). Advanced Methods of Microscope Control Using μManager Software. J. Biol. Methods *1*, e10. https://doi.org/10.14440/jbm.2014.36.
33. Schindelin, J., Arganda-Carreras, I., Frise, E., Kaynig, V., Longair, M., Pietzsch, T., Preibisch, S., Rueden, C., Saalfeld, S., Schmid, B., et al. (2012). Fiji: An Open-Source Platform for Biological-Image Analysis. Nat. Methods *9*, 676–682. https://doi.org/10.1038/nmeth.2019.

STAR★METHODS

KEY RESOURCES TABLE

REAGENT or RESOURCE	SOURCE	IDENTIFIER
Antibodies		
Alexa Fluor 647 goat anti-mouse IgG2A (Y2a)	Thermo Fisher Scientific	Cat# A-21241; RRID: AB_2535810
Anti-Hu CD3 biotin (MEM-57)	Exbio	Cat#10-202-C100; RRID: AB_10735443
Chemicals, peptides, and recombinant proteins		
3-amminopropyltriethoxysilane (APTES)	P-LAB	R.2328.1, CAS: 919-30-2
Polybead® amino microspheres, 0.112 µm	Polysciences, Inc.	
Qdot™ 525 ITK™ Amino (PEG) quantum dots	Thermo Fisher Scientific	Q21541MP
sulfo-NHS-biotin	CovaChem, LLC	14205-100; CAS: 119616-38-5
Streptavidin	Sigma	189730; UNIPROT: G7CCQ3
Dylight™ 649 streptavidin	BioLegend	405224
4-(bromomethyl)benzaldehyde	Merck	BL3H9538B038; CAS: 51359-78-5
Experimental models: Cell lines		
Jurkat cells, clone E6-1	ATCC	TIB-152
Recombinant DNA		
Plasmid: GCaMP6fu	Helassa et al.[25]	N/A
Plasmid: GCaMP6fast	Helassa et al.[25]	N/A
Software and algorithms		
Ossila contact angle v3.0.6.0	Ossila	https://www.ossila.com/products/contact-angle-goniometer
Gwyddion v2.60	Nečas et al.[28]	http://gwyddion.net/
ImageJ	Schindelin et al.[30]	https://imagej.nih.gov/ij/
CalQuo2 (variant CalQTrace)	Lee et al.[27]	https://www.bpi-oxford.com/home/software
µManager	Edelstein et al.[29]	https://micro-manager.org/

EXPERIMENTAL MODEL AND STUDY PARTICIPANT DETAILS

Cell lines

Jurkat cell (clone E6-1; ATCC) established from a male, acute T-cell leukemia patient were grown in RPMI-1640 medium (Fischer Scientific) supplemented with 10% of foetal bovine serum (Fischer Scientific), non-essential amino acids (Fischer Scientific) and 10mM HEPES under controlled humidity in the incubator at 37°C and 5 % CO_2. The cell line was regularly tested for morphology and mycoplasma infection. The cell line was authenticated using flow cytometry.

METHOD DETAILS

Contact angle measurement

Contact angle goniometer (Ossila Ltd, UK) was used to measure the contact angle in static mode at room temperature. A drop of deionized water was gently placed onto the surface (averages of n = 3 determinations) and analysed by Ossila contact angle software.

Atomic force microscopy

The topological images of the PS beads functionalized surface were achieved by A Nanosurf NaioAFM (Nanosurf, Switzerland), operated in dynamic AFM mode at room temperature. The imaging was performed using Dyn 190 Al tips in the measurement area of 10 µm ×10 µm and were zoomed in for getting more precise images. The images were collected at a scanning rate of 1 Hz with resolution of 512×512 points and were processed using Gwyddion software.[31]

Fluorescence microscopy

Fluorescence microscopy was performed on a home-built single-fluorophore sensitivity wide-field microscope with TIRF modality based on the IX71 body (Olympus). Fluorescence of QD QSA580 (Ocean NanoTech) was excited by 150 mW 405 nm laser (Cube, Coherent) and of Alexa Fluor™ 647 Conjugated streptavidin as well as IgG Alexa Fluor 647 antibody by 170 mW 638 nm laser (Lasos), respectively. All laser lines were focused to the back focal aperture of a 100x oil immersion TIRF objective (UApo N 100x, 1.49 NA, Olympus). TIRF illumination was achieved using a manual large-area translation platform (Thorlabs). Excitation and emission were separated through a filter-cube (Olympus) equipped with quadband beamsplitter (Chroma) and quadband emission filter (Chroma). Emission was additionally filtered out with 525/50 filter (Semrock) for Qdots, 605/70 or 655 LP (Chroma) for Alexa Fluor 647 positioned in front of EMCCD camera (iXon DU-897U, Andor). EM gain of the camera was set to 300, 100 images were acquired with the exposure time of 50 ms and summed in post-processing. Two acousto-optic tuneable filters (AOTFnC-400.650-TN, AA Optoelectronics) provided fast switching and synchronization of lasers with a camera. The whole system was controlled by μManager software.[29]

Chemical reagents & solutions

Ammonium hydroxide (NH_4OH), Ethanol (EtOH, UV grade), 3-aminopropyltriethoxysilane (APTES), Acetonitrile (ACN, UV grade), sodium cyanoborohydride ($NaBH_3CN$) (Penta Chemicals, Czech Republic), hydrogen Peroxide (H_2O_2) (Lach:ner, Czech Republic), molecule 1 (4-(bromomethyl)benzaldehyde) was purchased and used without further purification (Merck) Polybead® amino microspheres, 0.112 μm (Polysciences, Inc., Germany), Qdot™ 525 ITK™ Amino (PEG) quantum dots, sulfo-NHS-biotin, streptavidin, Dylight™ Fluor 649 streptavidin, Alexa Fluor 647 goat anti-mouse IgG2A (Y2a) (Thermo Fisher Scientific, USA), anti-Hu CD3 biotin (MEM-57, Exbio, Czech Republic), were purchased and used as received without further purification.

Ultrapure water was obtained in the laboratory using a Milli-Q water purification system. 1 mM solution of 4-(bromomethyl)benzaldehyde was prepared in acetonitrile and kept at room temperature. 1 μl in 5 ml was optimized as the concentration of nanoparticle solution and stored at 4°C. Just prior to use, different stock solutions of sodium cyanoborohydride (13 mg) and biotin (2 mg) were prepared in 300 μl and 1000 μl of water, respectively. 0.5% BSA in PBS was used to prepare streptavidin and antibody solutions and to prevent non-specific interactions of the molecules with the surface. Sodium acetate buffer (0.2 M, pH 4.5) was prepared by dissolving sodium acetate trihydrate in distilled water; the final pH was adjusted by acetic acid (0.2 M). Phosphate-buffered saline, 10×PBS contains 80 g sodium chloride, 2 g potassium chloride, 14.4 g disodium hydrogen phosphate and 2.4 g potassium dihydrogen phosphate in 1 litre of Milli-Q water. The mixture was sterilized by autoclaving, stored at room temperature and diluted 10× prior to use to get 1×PBS used throughout the study. Bovine serum albumin, BSA, solutions were prepared by directly dissolving BSA in 1×PBS. It was kept at 4°C. All buffers were filtered through 0.22 μm nylon membrane filter.

Surface functionalization

Cleaning

In terms of high-resolution imaging, biocompatibility as well as degradability, optical coverslips (25 mm) are selected as an ideal platform for fabricating the multilayer system. The cleaning methods include the sonication of coverslips in ultrapure water, acetone, and isopropyl alcohol, consecutively for 10 minutes. After washing and heating at 80°C in diluted basic Piranha solution (5:1:1 v/v mixture of water, 26% aqueous ammonia and 30% aqueous hydrogen peroxide, respectively) for 20 minutes, the coverslips are rinsed with distilled water and dried.

Amino silanization

The cleaned coverslips were placed in a petri dish with 3% APTES solution in ethanol at room temperature. After 20 minutes, the surface was thoroughly rinsed with ethanol and dried completely.

Treatment with 4-(bromomethyl)benzaldehyde

The APTES modified substrate was kept in solution of 4-(bromomethyl)benzaldehyde for 45 minutes, followed by washing with distilled water and drying. See Figure S1 for images of the contact angle after cleaning, silanization and treatment with 4-(bromomethyl)benzaldehyde.

Functionalization with PS beads and Qdots

The nanoparticle solution (200 μl) followed by $NaBH_3CN$ (300 μl) were separately pipetted on the aldehyde functionalized surface at room temperature for 45 minutes. After washing and drying, the coverslip was immersed in acetate buffer for 30 minutes. Then the surface was subsequently washed with distilled water and dried. See Figure S2 for the fluorescence images of the Qdots functionalized coverslip.

Bioconjugation with biotin-streptavidin

Biotinylation was achieved by adding 300 μl of the biotin solution onto the nanoparticle functionalized surface for 30 minutes at room temperature. Afterwards, the surface was washed with water, methanol, and water. Finally, the coverslips were incubated in 1% BSA-1×PBS at 37°C for 1 h to block the non-specific binding site. After washing with water, the nanosurface was incubated with 300 μl of unlabelled

streptavidin solution (10 ng/ml) at room temperature for 30 minutes, followed by washing with 300 μl of 0.5% BSA in PBS (5×3 minutes). See Figure S3 for the fluorescence images of nanoparticles covered surface functionalized with streptavidin.

Antibody immobilization

The antibody immobilization was performed by exposing the functionalized surface to 300 μl of antibody solution on parafilm for 30 minutes at room temperature. After incubation, the surface was thoroughly washed with 0.5% BSA in PBS (5×3 minutes) and another blocking with 5% BSA in PBS at 37°C for 30 minutes. See Figure S4 for the fluorescence images of the surface after binding the antibody.

Transfection

For the expression of GCaMP6fu and GCaMP6fast genetically encoded calcium probes, Jurkat cells were transiently transfected with DNA plasmids using the Neon® transfection system (Thermo Fisher Scientific). The transfection was performed using 1 μg of the DNA plasmid and 300,000 cells in 0.5 ml of pre-warmed supplemented RPMI-1640 culture medium. The instrument settings were 3 pulses, each 1500 V for 10 ms. The cells were incubated for 16-24h before imaging.

Single-cell calcium measurement

The coverslips were mounted to the ChamLide imaging chamber, and the cells were transferred to the coverslip as previously described for the large-scale calcium measurement. Cells transfected with genetically encoded calcium probe GCaMP6fast were imaged using a home-built super-resolution wide-field TIRF microscope described in fluorescence microscopy section in the methods. The imaging was performed in the TIRF mode using the 488 nm laser with a 5% power intensity; the emission was filtered using 525/50 filter (Semrock) positioned in front of the EMCCD camera (iXon DU-897U, Andor). EM gain of the camera was set to 100 with an exposure time of 100 ms; individual cells were imaged for at least 15 min. The calcium influx was analysed by the mean fluorescence intensity (MFI) changes of the cells landing on the coverslips for at least 10 minutes. The area occupied by the landing cell was selected manually. The peak intensity was determined by finding the maximum MFI, the MFI after 5 min and 10 min, the values were used to determine the kinetics of fluorescence decay. Higher values indicate a more rapid decay of the fluorescence, which indicates more active response.[21]

QUANTIFICATION AND STATISTICAL ANALYSIS

Large-scale calcium measurement

The functionalized coverslips were mounted in a ChamLide holder (Live Cell Instruments) with a microfluidics system and kept in 500 μl of PBS-BSA 5%, attached in a live-cell environmental chamber (Uno, Okolab S.r.l.) at 37°C for the entire experiment.

A day after transfection, 600.000 cells were centrifuged for 3 min at 0.3 rcf and resuspended in 1 ml of pre-warmed colour-free RPMI-1640 supplemented with 10% of foetal bovine serum (Fischer Scientific), non-essential amino acids (Fischer Scientific), 1 mM $CaCl_2$ and 1 mM $MgCl_2$. Immediately after resuspension, the cells were transferred to the coverslip using the microfluidics system, with the image acquisition running shortly before.

Live-cell calcium influx measurements were performed on the IX73 frame (Olympus) equipped with ×20 objective (UPLXAPO20X, Olympus), LED epifluorescence illumination system (CoolLED pE-4000, CoolLED) and sCMOS camera (Zyla 4.2P-CL10, Andor). Coated coverslips were mounted into the ChamLide holder with a microfluidics system attached to a live-cell environmental chamber (Uno, Okolab S.r.l.) set to 37°C. The acquisition time for one frame was 250 ms with illumination using 470 nm laser set to 10%. Cells were imaged for 15 min (3600 frames) after injection into the imaging chamber. The acquisition was controlled by μManager software (ver. 1.4.24).[32]

Data analysis. Obtained data were converted to 8-bit mode and processed to have a minimum intensity of 20-35 using Fiji/ImageJ software (version 1.53f51),[33] not affecting the brightness of the cells and evenly reducing the background variations. The data was saved and uploaded to the novel AI-algorithm CalQTrace (unpublished) based on the previously reported algorithm CalQuo2[30] to calculate the calcium response of single cells. The algorithm was set to detect cells with a diameter of 24-26 pixels and with a brightness slightly higher than the minimal background. Single cells were tracked for at least 1500 frames (6 min, 15 sec), and the algorithm classified the cells depending on variations of their normalized intensity. Five independent experiments were performed (Tables S1 and S3). The n represents the number of cells detected during the image analysis. Statistical differences were evaluated using unpaired T-test; *P < 0.05 (GraphPad Prism 9). See Table S2 and Figure S6 for detailed statistical differences.